Visual Abstract

Detection of uniaxial fatigue stress under magnetic flux leakage signals using Morlet wavelet

S.M. Firdaus, A. Arifin, S. Abdullah, S.S.K. Singh
Department of Mechanical and Manufacturing Engineering, Faculty of Engineering and Built Environment, Universiti Kebangsaan Malaysia, 43600 UKM Bangi, Selangor, Malaysia.
syedmuhdfirdaus96@gmail.com, azli@ukm.edu.my, shahrum@ukm.edu.my, salvinder@ukm.edu.my

N. Md Nor
Civil Engineering Studies, College of Engineering, Universiti Teknologi MARA, Cawangan Pulau Pinang, 13500 Permatang Pauh, Pulau Pinang, Malaysia.
ida_nsn@uitm.edu.my

ABSTRACT. This paper demonstrates the application of continuous wavelet transform technique for magnetic flux leakage signal generated during a uniaxial fatigue test. This is a consideration as the magnetic signal is weak and susceptible to being influenced by an external magnetic field. The magnetic flux leakage signal response of API steel grade X65 is determined using Metal Magnetic Memory under cyclic load conditions ranging from 50% to 85% of the UTS. To facilitate further signal analysis, the magnetic flux gradient, the dH(y)/dx signal were converted from a length base into time series in this study. Magnetic flux leakage readings indicated a maximum UTS load of 56.5 (A/m)/mm at 85%, where a higher load resulted in a higher reading and the signal contained Morlet wavelet coefficient energy of 1.02×106 μe^2/Hz. As increasing percentages of UTS loads were applied, the signal analysis revealed an increasing linear trend in the dH(y)/dx and wavelet coefficient energy. The analysis revealed a strong correlation between the wavelet coefficient energy and the dH(y)/dx amplitude, as indicated by the coefficient of determination (R^2) value of 0.8572. Hence, this technique can provide critical information about magnetic flux leakage signals that can be used to detect high stress concentration zones.

KEYWORDS. Ferromagnetic Steel; Metal Magnetic Memory; Wavelet Transform; Uniaxial Fatigue Stress.

OPEN ACCESS

Citation: Firdaus, S.M., Arifin, A., Abdullah, S., Singh, S.S.K., Nor. N. Md. Detection of uniaxial fatigue stress under magnetic flux leakage signals using Morlet wavelet, Frattura ed Integrità Strutturale, 61 (2022) 254-265.

Received: 15.02.2022
Accepted: 30.04.2022
Online first: 01.07.2022
Published: 01.07.2022

INTRODUCTION

Oil and gas are delivered across pipelines by pump stations positioned along the pipeline; these, are considered long-term facilities in the petroleum industry. Regardless, failures are almost always the result of human error as a result of design negligence during construction or operation [1]. The operational condition of pipelines can also contribute to their failure through factors such as temperature variation, frequency, and cyclic stress; these factors are particularly detrimental to above-ground pipelines [2,3]. To minimise the risk of system failure, accurate analysis of structures with a long service life, such as pipelines, is required. Therefore, non-destructive testing (NDT) methods are frequently used in the engineering industry to monitor and control the occurrence of defects. Due to the fact that NDT does not alter the object's original state, it is a critical diagnostic mechanism for assessing environmental impacts, material properties, and previous interferences [4].

Conventional NDT techniques, such as Eddy current testing (ET), ultrasonic testing (UT), and magnetic particle testing (MT), can only measure macroscopic defects of a certain size, but are limited in their ability to detect early damage and dynamic monitoring [5]. A great number of non-destructive magnetic techniques have been developed over the last decade regarding to its physical basis to evaluate the stress status of ferromagnetic structures such as magnetic Barkhausen noise, magnetoacoustics emission, and stress-induced magnetic anisotropy [6]. Magnetic NDT technologies have been extensively adopted in engineering to ensure the operating safety of ferromagnetic structures and components, but the presence of an external magnetic field is a necessary condition to operated [7,8]. To address this issue, a Russian researcher developed a new magnetic testing technique called the metal magnetic memory (MMM) technique, which has generated considerable interest [9]. In comparison to other magnetic testing methods, the MMM method has a number of advantages, particularly its passive testing method, which evaluates the self-magnetic flux leakage (SMLF) signal produced by ferromagnetic materials and paramagnetic products at high density dislocations [10]. Moreover, the residual magnetic field can be measured using the MMM method, which is stimulated by mechanical stress in conjunction with the geomagnetic field without requiring artificial magnetisation and has demonstrated its utility in monitoring early damage development [11].

However, the magnetic sensor signal is weak and susceptible to noise, interference, and undesirable magnetic signals from the environment [12]. Signal processing in the time-frequency domain analysis is now frequently used to extract indistinguishable hidden signal information from the original signal. Due to its more flexible features, the Wavelet transform is preferred over the short-time Fourier transform in time-frequency domain analysis [13]. This paper aims to define the attribution associated with uniaxial fatigue loading by processing the magnetic flux leakage signals using the continuous wavelet transform. The dH(y)/dx value and the Morlet wavelet coefficient energy of the magnetic flux leakage signals are hypothesised to have a strong correlation. This analysis aids in the identification of stress concentration zones in pipeline durability assessments.

EXPERIMENTAL PROCEDURE

Fig. 1 illustrates the overall framework for this study. The material used was ferromagnetic steel grade X65 in accordance with the American Petroleum Institute (API), which is frequently used in the oil, gas, and petrochemical industries [14]. The specimen was fabricated in accordance with ASTM-08, as shown in Fig. 2 (Standard Test Method for Tension Testing of Metallic Materials), in order to obtain its monotonic properties via tensile testing at ambient temperature. The strain rate value was set at 1×10^{-3}/second in this tensile test.

A cyclic uniaxial fatigue test was conducted on a servo hydraulic machine with a capacity of 25 kN in accordance with ASTM E466 (Standard Practice for Conducting Force Controlled Constant Amplitude Axial Fatigue Test of Metallic Materials), as illustrated in Fig. 3. The specimen was subjected to uniaxial fatigue tests with loads ranging from 50% to 85% of the API steel grade X65's Ultimate Tensile Strength (UTS) to determine how load variation affects the magnetic signals. The stress ratio was set to 0, the minimum forces applied were 0, and the maximum forces were proportional to the percentage of UTS loads. Then, magnetic flux leakage signals were measured using the MMM scanning device, as shown in Fig. 4, to determine the location of the specimen's high stress concentration area [15]. During the fatigue test procedure, the type 2-2 sensor equipment was used to scan the SMLF response data or signals. The lift-off rate was set to 0 mm, and the distance between the centre point of the wheels and the sensor was set to 5 mm. In this study, the magnetic flux leakage signal response was measured using the distance mode. Then, data was obtained by rolling the MMM scanning device along an 80-mm scanning line, as illustrated in Fig. 2, since this region was within the expected failure occurrence range. The specimen was subjected to the cyclic test until it failed completely. The remaining load conditions were treated similarly.

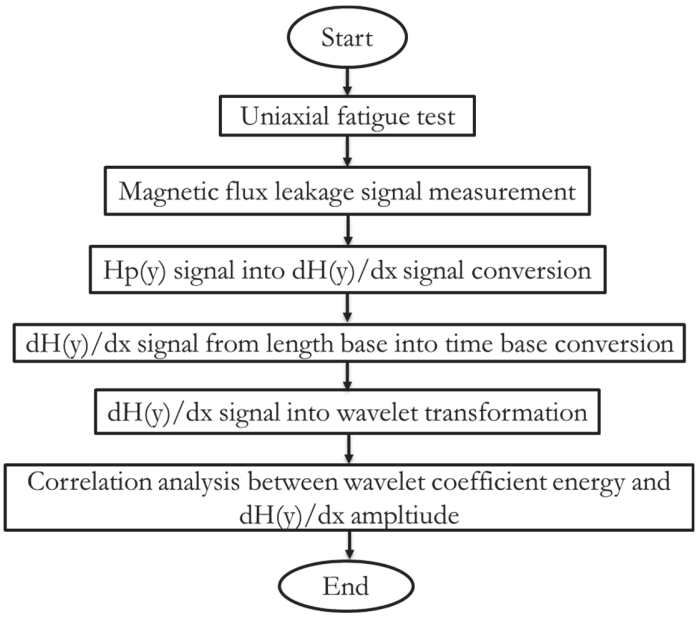

Figure 1: Process flow for signal analysis of the magnetic flux leakage signal.

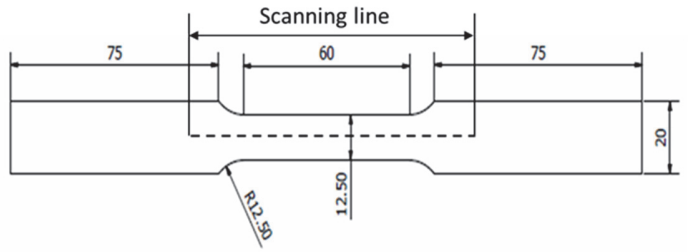

Figure 2: API steel grade X65 specimen (dimension in mm) with scanning line for MMM data acquisition.

Figure 3: Experiment setup for cyclic test.

(a) (b)

Figure 4: MMM data acquisition; a) device and b) procedure.

THEORETICAL FRAMEWORK

The two parameters used in the MMM technique to detect magnetic flux leakage responses located in stress concentration zones are the normal segment, Hp(y), and the tangential segment, Hp(x) of magnetic intensity signals. In this study, the normal segment of magnetic intensity, Hp(y), was used because it provided the best evaluation in terms of damage exposure [16]. The acquired raw signals, normal component of magnetic intensity, Hp(y), were converted to the gradient component of magnetic intensity signals, dH(y)/dx, both in length-based forms. The dH(y)/dx signals were chosen for further analysis as they were capable of showing the severity level of detected defects on the scanned specimen's surface. The dH(y)/dx signals were then converted from length-based into time-based in line with the MMM acquisition concept at a rate of 10 min/mm [17], as reported by [18], to enable their transformation into the time-frequency domain. The wavelet transform approach is apparently one of the most widely used time-frequency techniques for overcoming nonstationary signals by dividing the time domain into different frequency segments using time and frequency alterations. This approach provides data in a more usable way in both the time and frequency domains [19].

The wavelet transform begins with the selection of a basic function, also referred to as the mother wavelet, which scales and translates the signal in order to analyse it. It determines the spectrum for each location by adjusting a window along the signal, which ultimately represents the time-frequency signal with multiple resolutions and simultaneously provides time and frequency information about an event. The Morlet wavelets are a subclass of mother wavelets that are frequently used in the analysis of the Continuous Wavelet Transform (CWT). The coefficients are computed by the wavelet decomposition as a similarity index between the signal and the processed wavelet, which is the result of a regression of an original signal composed of distinct scales and distinct segments on the wavelet. It denotes the relationship between the wavelet and a signal segment. The similarity is strong if the index is large; otherwise, it is minor [20, 21]. The wavelet transform of any time-shifting signal, f(t), is described as the quantity of all the signal time multiplied by a scaled and shifted interpretation of the wavelet function ψ(t) [22]. The CWT is defined by the following integral:

$$CWT_{(a,b)} = \int_{-\infty}^{+\infty} f(t)\Psi_{a,b}(t)dt \tag{1}$$

where a and b are the scale factors and $\psi_{(a,b)}$ is the mother wavelet. The scale index, which is a reciprocal frequency, is represented by parameter a, whereas parameter b indicates time shifting. The following integral is used to express the CWT's wavelet coefficient [23].

$$WC_{(p,q)} = \frac{1}{\sqrt{p}} \int_{-\infty}^{+\infty} F_{(t)}\Psi\left(\frac{t-q}{p}\right)dt \tag{2}$$

The similarity index, i.e., coefficient, between the evaluated signal and the generated wavelet is obtained through wavelet decomposition as shown in Eqn. 2, where p is the scale index, F is the signal amplitude and q is the time shifting. The scaling factor allows controlling the shape of the basic wavelet and balances the time and frequency resolutions. Decreasing the scale index increases the frequency resolution but decreases the time resolution. When the scale index tends to zero, the wavelet becomes a cosine function which has the finest frequency resolution, and when it tends to infinity, the wavelet has the finest time resolution. In the time-frequency domain, the wavelet coefficient describes the signal's energy distribution. The internal energy contained in the signal can be defined as follows [24].

$$e_{(p,q)} = \int_{-\infty}^{+\infty} \left| WC_{(t)} \right|^2 dt \tag{3}$$

In this study, the energy distribution was decomposed into the time domain spectrum using Eqn. (3) by obtaining the magnitude of the cumulative value for each time section. The energy was then used to ascertain changes in the amplitudes of the strain signals.

RESULT AND DISCUSSION

Tensile tests conducted on API X65 steel yielded monotonic properties, as shown in Tab. 1. The UTS was chosen in this study to design the load for uniaxial fatigue testing with a value of 572 MPa divided into eight different types of loads ranging from 50% to 85% of the UTS load. From the data acquired during the fatigue test, the Hp(y) signal response indicated an increase in magnetic intensity between 60 mm and 70 mm, which corresponded to the location of the failed specimen highlighted by the red circle, as shown in Fig. 5. According to the figure, 85% of the UTS load resulted in the highest reading of magnetic intensity, which gradually decreased to 75% until 50% of the UTS load. Then, Hp(y) signals were converted to dH(y)/dx signals, as illustrated in Fig. 6, since they are preferred over normal component signals for being more responsive to damage intensity in detecting high stress concentration zones. The recorded dH(y)/dx signals indicated increasing amplitude values from 50 % to 85 % of the UTS load, as the load variation itself affected the magnetic flux leakage readings. Significant variations in the dH(y)/dx signals were also measured similarly. Significant variations in the dH(y)/dx signals were also measured at same locations of scanning line as Hp(y) signals, the steep peaks at 60 mm – 75 mm from 50 % until 85 % of UTS. Magnetic field leakage occurred at the stress concentration position as a result of irreversible changes in the magnetic domain orientation; these changes can be attributed to the magnetic field-induced operating stress [25]. The high peaks of the dH(y)/dx values within these areas were expected, as the high concentration zone is where the specimen was damaged prior to failure.

Properties	Values
Yield strength (MPa)	572
Ultimate tensile strength (MPa)	614
Young's modulus (GPa)	220

Table 1: Monotonic properties of API steel X65.

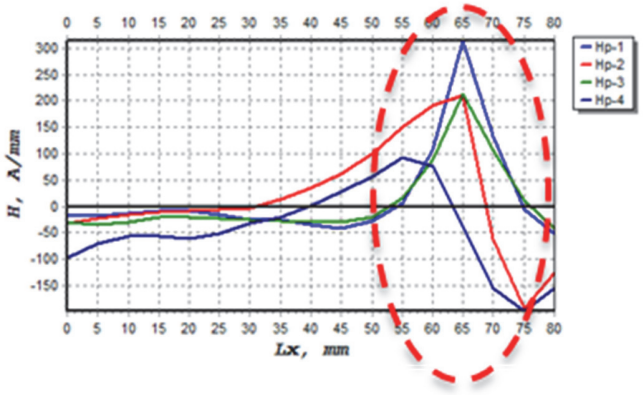

a) 85 % UTS

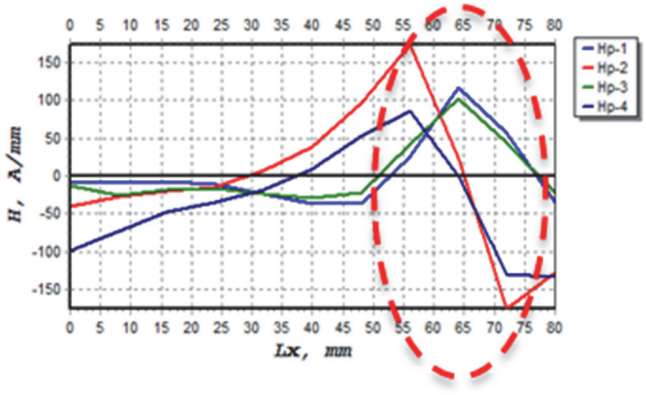

e) 80 % UTS

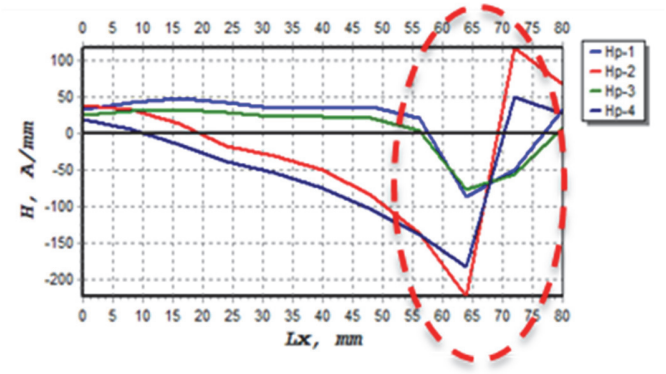

b) 75 % UTS

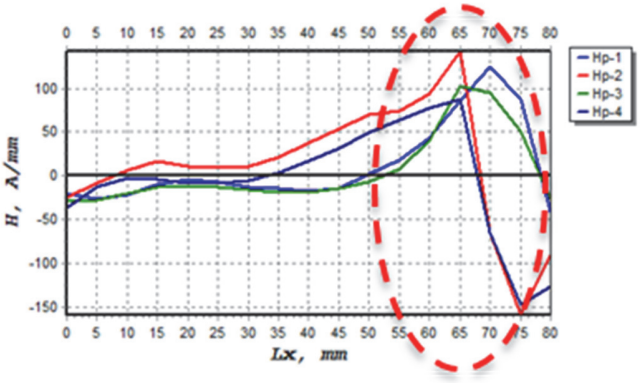

f) 70 % UTS

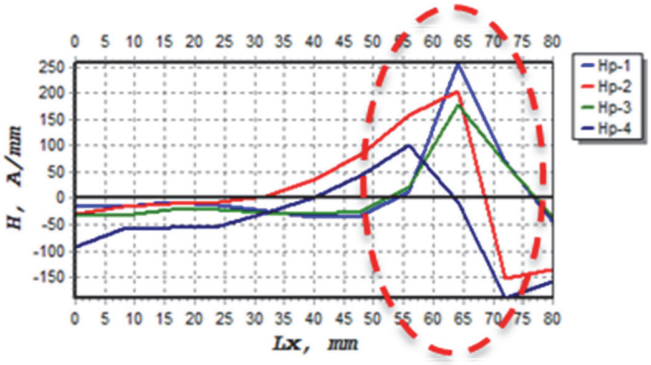

c) 65 % UTS

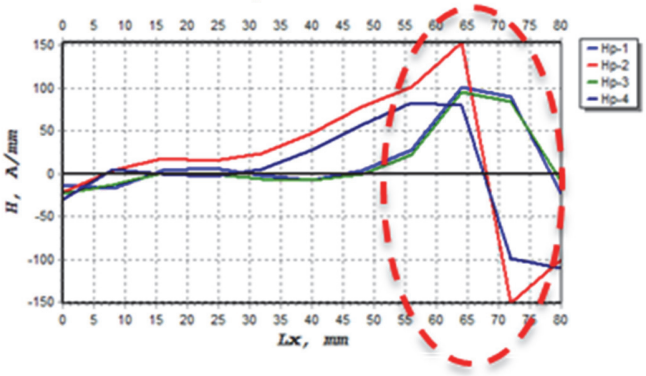

g) 60 % UTS

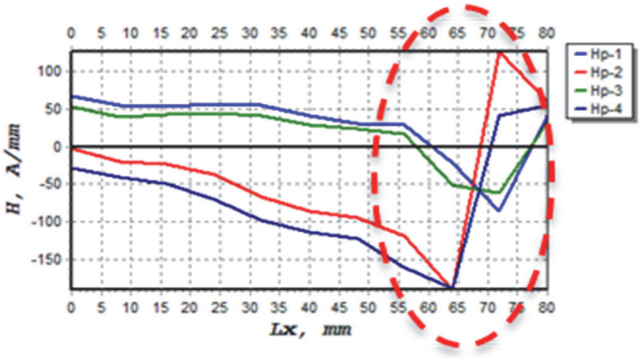

d) 55 % UTS

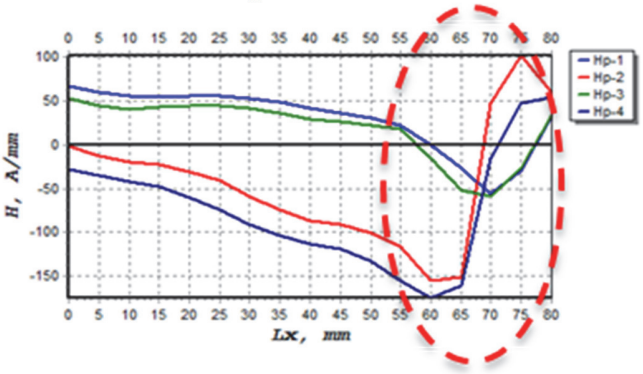

h) 50 % UTS

Figure 5: Magnetic intensity response from the UTS loads of; a)85%, b)80%, c)75%, d)70%, e)65%, f)60%, g)55% and h)50%.

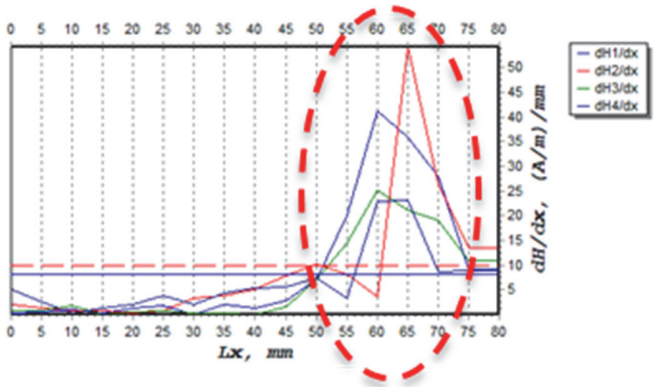

a) 85 % UTS

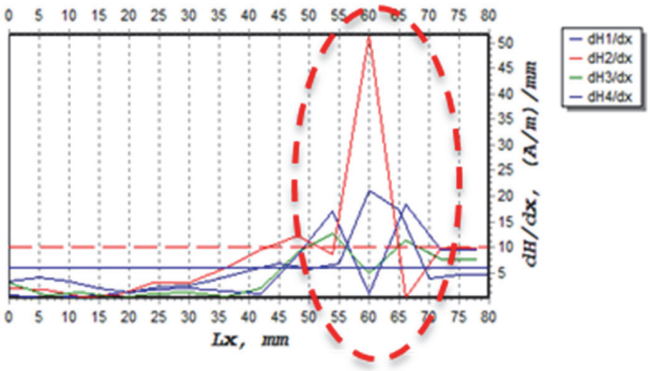

b) 80 % UTS

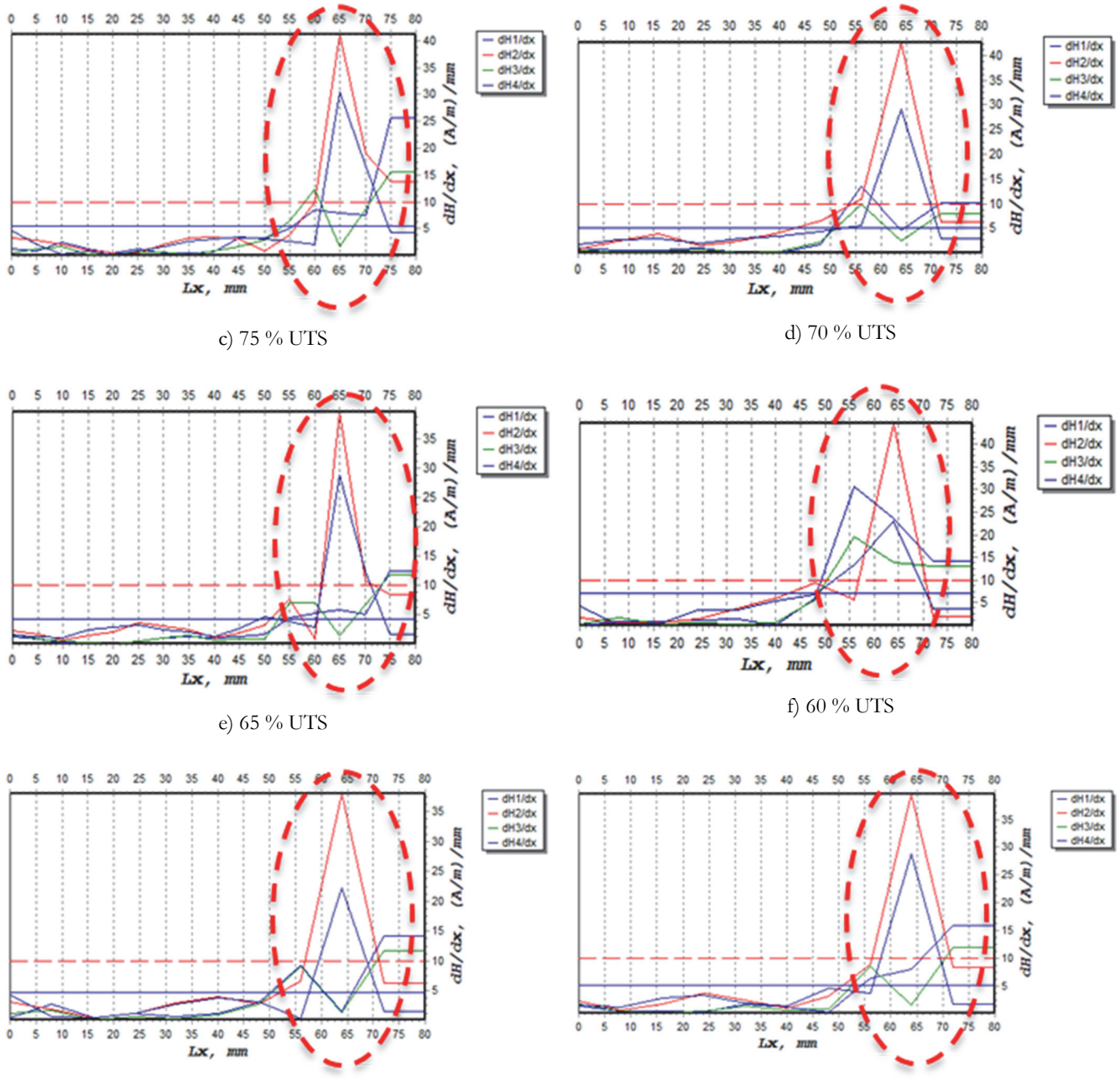

c) 75 % UTS

d) 70 % UTS

e) 65 % UTS

f) 60 % UTS

g) 55 % UTS

h) 50 % UTS

Figure 6: Gradient of magnetic intensity response from UTS loads of; a)85%, b)80%, c)75%, d)70%, e)65%, f)60%, g)55% and h)50%.

The values of the dH(y)/dx signal can be used to determine the stress concentration zone. Ferromagnetic materials can produce spontaneous magnetic signals that can very likely be used to assess the extent of damage due to the effect of stress. However, at a scanning distance of 0 to 60 mm, the MMM scanning device sensors identified several additional dH(y)/dx signals. Because no substantial changes were observed, these signals were not examined in this investigation. The sensor identified these signals by analysing the impact of the ambient and initial magnetic fields from the fatigue testing machine clamps.

As illustrated in Fig. 6, the raw signals obtained from the magnetogram were in the modulus state, with all values being positive, indicating that the stress level had been properly classified. Next, all the dH(y)/dx channels were converted into time series, as shown in Fig. 7. The y-axis remained at a constant value, whereas the x-axis changed from the 80 mm length-based to the 8 s time-based, making it more appropriate to employ additional signal processing techniques. All signals that increased from 50% to 85% of the UTS load in the time domain showed that their highest amplitudes were similar to the

defect locations, as shown in Fig. 5 and Fig. 6. This obviously indicated that the highest peaks were within the range of 6 s to 8 s due to the expected region of specimen failure.

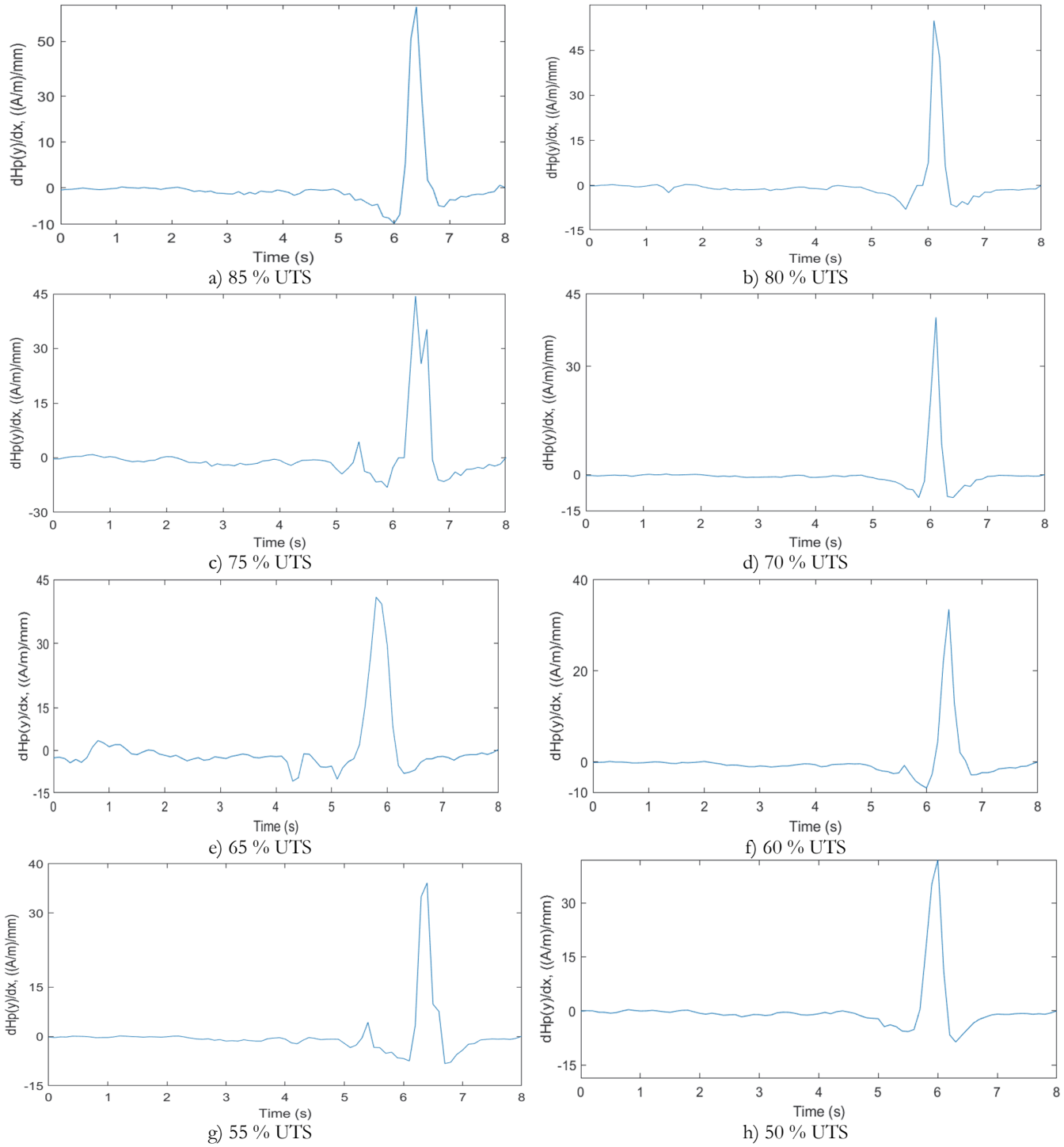

Figure 7: Time base magnetic flux leakage signals from UTS loads of; a)85%, b)80%, c)75%, d)70%, e)65%, f)60%, g)55% and h)50%.

Then, after the conversion of the dH(y)/dx signals from length-based to time-based, the MMM signals were transformed into the time-frequency domain since the Morlet wavelet transform was chosen as the basic function for the transformation. As illustrated in Fig. 8, the estimation of wavelet coefficients was the first step in a wavelet analysis, as the matrix row (x-axis) represents the time parameter and the matrix column (y-axis) represents the scale parameter, which is inversely

proportional to the frequency in scalogram displays. In the time-frequency domain, the wavelet coefficients represent how the energy of the magnetic flux leakage signals is divided. The magnitude of colors corresponds to the absolute wavelet coefficient values as they indicate the energy distribution features with respect to time and frequency. At a higher frequency and with a lower amplitude on the scalogram, a smaller scale indicates that the cycles have more energy, indicating a tendency to cause failure events.

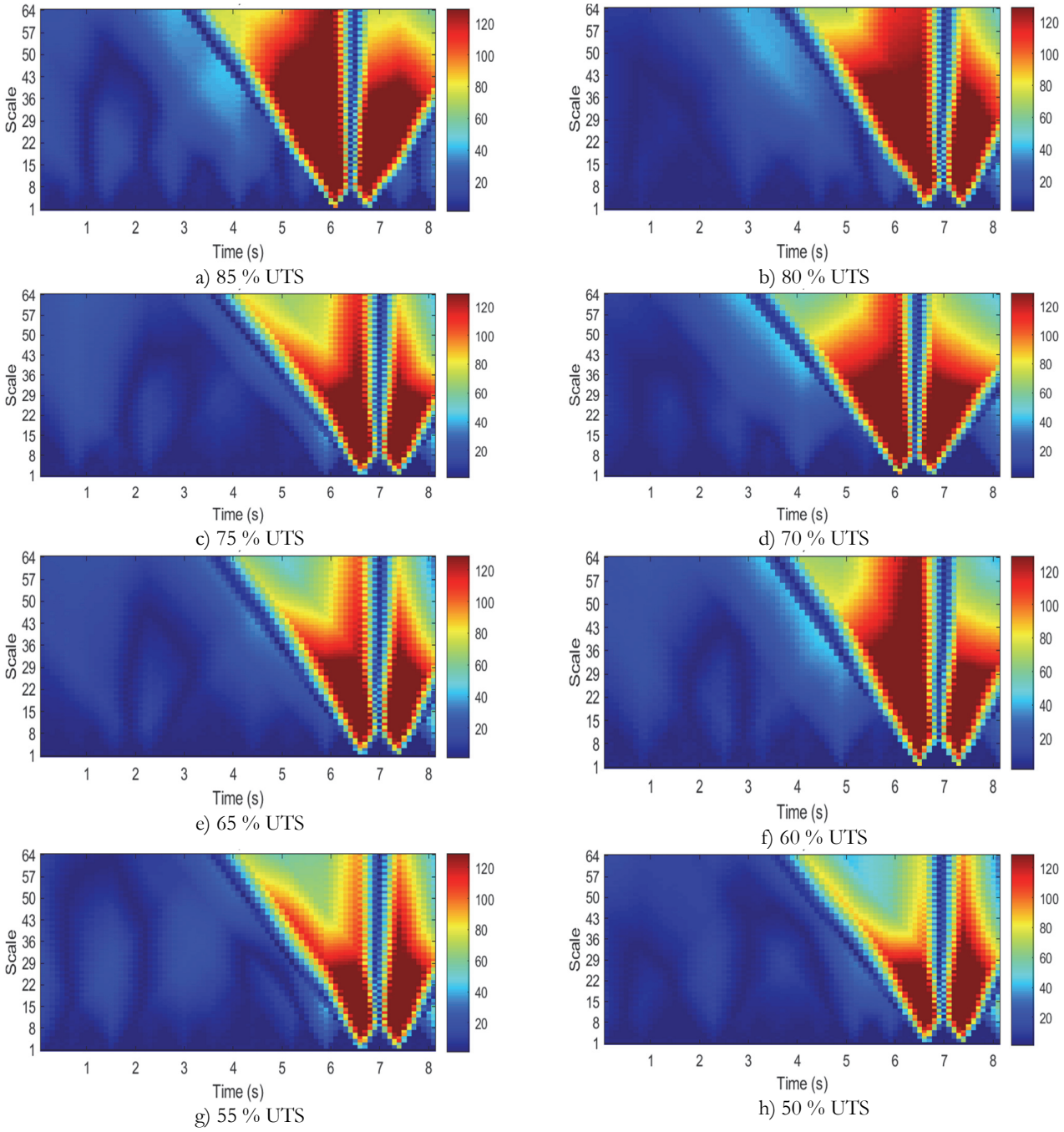

Figure 8: Wavelet coefficient distribution plot of collected MMM signals.

From these energy-based distribution plots, it was observed that similar locations of high amplitude features were detected for 50% to 85% of the UTS load signals based on the related coefficients, indicating the dominant energy at 4 s to 8 s. Evidently, the lower the frequency, the larger the magnitude distributions: conversely, the lower the magnitude distribution, the higher the frequency of events. These large magnitude distributions in the signals corresponded to zones of high stress

concentration or failure occurrences. The signal contained the least energy at 50% of the UTS load, with a value of 2.49×10^5 $\mu e^2/Hz$, and the remaining UTS load signals contained the most energy at 85% of the UTS load, with a value of 1.02×10^6 $\mu e^2/Hz$, as tabulated in Tab. 2 along with the values of dH(y)/dx amplitudes. The overall wavelet coefficient energy obtained from the magnetic flux leakage according to each UTS load from 50% to 85% shown in Fig. 9. Based on the results, the wavelet coefficient energy shows increasing trend along with increment of UTS loads except for 60% and 70%. This is due to disturbance magnetic signal reading from environmental during data measurement. Thus, the variation most of the loads for UTS percentage influences the total energy contained in the signals.

UTS, (%)	Stress, MPa	dH(y)/dx amplitude, ((A/m)/mm)	CWT coefficient energy, ($\mu e^2/Hz$)
50	307.0	35.9	2.49×10^5
55	337.7	42.6	3.29×10^5
60	368.4	48.3	5.13×10^5
65	399.1	47.9	4.51×10^5
70	429.8	52.3	6.23×10^5
75	460.5	54.4	6.08×10^5
80	491.2	54.2	7.78×10^5
85	521.9	56.5	1.02×10^6

Table 2: Value of dH(y)/dx readings and CWT coefficient energy.

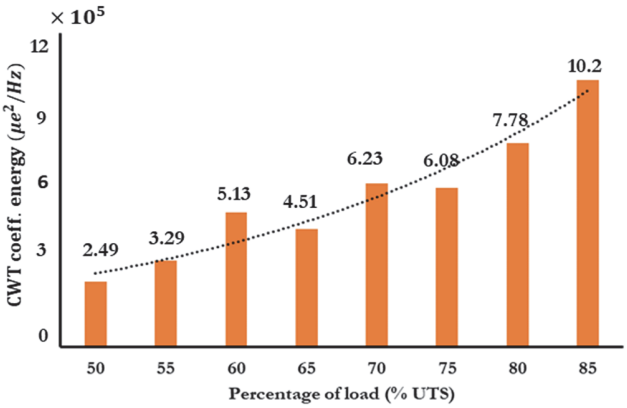

Figure 9: Characterisation of wavelet coefficient energy toward percentage of loads applied.

Finally, Fig. 10 shows that the wavelet coefficient energy correlated to the amplitude of the dH(y)/dx signals. The power law correlation was applied to quantify the correlation between these two parameters and show a relationship with coefficient of determination (R^2) value of 0.8572 as in the Fig. 10 which represents the suitability of the data fitting. Higher R^2 values indicate greater fitness of the regression with the data. When the prediction is poor, uncertainty or error shall reflect a significance value of the prediction. Although the R^2 value of this correlation was under excellent correlation which was 0.9, but it still considered as acceptable correlation as it above the value of 0.8 [26]. A good correlation indicates the prediction results are closely associated with the experimental data. The pattern reveals that the dH(y)/dx amplitudes was generally converted into energy loss, with the dH(y)/dx amplitudes decreasing as energy was lost following the reducing of UTS loads. Signal with high amplitudes represented a higher energy distribution in the signals. This energy spectrum gained form continuous wavelet transform was shown to be relatively effective in detecting high amplitude of fatigue events in magnetic flux leakage signals response and was a highly effective tool for detecting high stress concentration zones. This developed signal processing technique can be implemented to determine the possible locations of defects even if defect characteristics are no quantitively defined. These wavelets can also be used to perform local analysis and thus can analyse a localised area of a large signal in durability assessment.

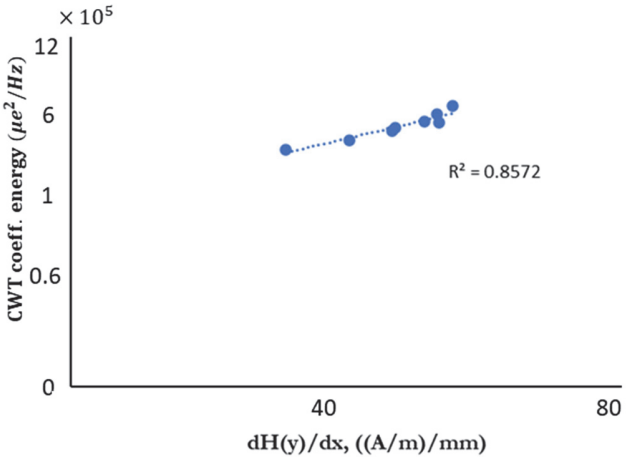

Figure 10: Correlation between energy contained in the signals and the dH(y)/dx amplitude.

CONCLUSION

In this study, the MMM method was used to determine the wavelet coefficient energy of API steel grade X65 in response to magnetic flux leakage during uniaxial fatigue testing. Uniaxial fatigue testing was conducted with loads ranging from 50% to 85% of the API steel grade X65's UTS value. Accordingly, it was determined that increased fatigue loading resulted in MMM readings and signals with high energy content. The results indicate that a 85% UTS load resulted in the highest readings of the dH(y)/dx amplitude and wavelet energy contained in the signal, which were 56.5 (A/m)/mm and 1.02×10^6 με²/Hz, respectively. The wavelet coefficient produced an energy distribution with a similar pattern to that of the dH(y)/ dx signal at the same event localisation. From the power law regression, the Morlet wavelet coefficient energy showed a positive correlation, with an R^2 value of 0.8572. These findings indicate a strong link between the wavelet coefficient energy and the dH(y)/dx amplitude. Therefore, the proposed use of the dH(y)/dx ratio in time series to extract features in the time-frequency domain via wavelet transform is recommended for durability assessments.

ACKNOWLEDGEMENT

The authors wish to acknowledge to the Ministry of Higher Education (FRGS/1/2018/TK03/UKM/02/1) and Universiti Kebangsaan Malaysia (DIP-2019-015) for the grant research support.

REFERENCES

[1] Chen, X., Wu, Z., Chen, W., Kang, R. & He, X. (2019). Selection of key indicator for reputation loss in oil and gas pipeline failure event, Engineering Failure Analysis, 99, pp. 69-84. DOI: 10.1016/j.engfailanal.2019.01.071

[2] Hredil, M., Krechkovska, H., Tsyrulnyk, O. and Student, O. (2014). Fatigue crack growth in operated gas pipeline steels, Procedia Structural Integrity., 26, pp. 409-416. DOI: 10.1016/j.prostr.2020.06.052

[3] Mansor, N.I.I., Abdullah, S. and Ariffin, A.K. (2019). Effect of loading sequences on fatigue crack growth and crack closure in API X65 steel, Marine Structures, 65, pp. 181-196. DOI: 10.1016/j.marstruc.2019.01.007

[4] Işık, N., Halifeoğlu, F. M. and İpek, S. (2020). Nondestructive testing techniques to evaluate the structural damage of historical city walls. Construction and Building Materials, 253. DOI: 10.1016/j.conbuildmat.2020.119228

[5] Wang, Z.D., Gu, Y. & Wang, Y.S. (2012). A review of three magnetic NDT technologies. Journal of Magnetism dan Magnetic Materials, 324, pp. 382-388. DOI: 10.1016/j.jmmm.2011.08.048

[6] Zhao, X., Su, S., Wang, W. and Zhang, X. Metal magnetic memory inspection of Q345B steel beam in four point bending fatigue test. Journal of Magnetism and Magnetic Materials, 514, pp. 167155. DOI: 10.1016/j.jmmm.2020.167155

[7] Su, S., Yang, Y., Wang, W. and Ma, X. Crack propagation characterization and statistical evaluation of fatigue life for locally corroded bridge steel based on metal magnetic memory method. Journal of Magnetism and Magnetic Materials, 536, pp. 168136. DOI: 10.1016/j.jmmm.2021.168136
[8] Moonesan, M. and Kashefi. M. (2018). M. Effect of sample initial magnetic field on the metal magnetic memory NDT result. Journal of Magnetism and Magnetic Materials, 460, pp. 285-291. DOI: 10.1016/j.jmmm.2018.04.006
[9] Shi, P., Jin, K. and Zheng, X. (2017). A magnetomechanical model for the magnetic memory method. International Journal of Mechanical Sciences, 124–125, pp. 229–241. DOI: 10.1016/j.ijmecsci.2017.03.001
[10] Dubov, A.A. (2014). Energy diagnostics-is a physical basis of the metal magnetic memory method. 11th European Conference on Non-Destructive Testing. ECNDT: pp. 1-8.
[11] Hu, Z., Fan, J., Wu, S., Dai, H. and Liu, S. (2018). Characteristics of metal magnetic memory testing of 35CrMO steel during fatigue loading. Metals, 8(2). DOI: 10.3390/met8020119
[12] Liu, B., He, L., Zhang, H., Sfarra, S., Fernandes, H., Perilli, S. and Ren, J. (2019). Quantitative study of magnetic memory signal characteristic affected by external magnetic field. Measurement: Journal of the International Measurement Confederation, 131, pp. 730–736. DOI: 10.1016/j.measurement.2018.09.025
[13] Zhang, M., Li, M., Zhang, J., Liu, L. and Li, H. (2020). Onset detection of ultrasonic signals for the testing of concrete foundation piles by coupled continuous wavelet transform and machine learning algorithms. Advanced Engineering Informatics, 43. DOI: 10.1016/j.aei.2020.101034
[14] Mousavi, S.H., Arab, Gh., Sabzi, M., Sadeghi, M., Eivani, A.R. and Jafarian, H.R. (2021). Sensitivity to hydrogen induced cracking, and corrosion performance of an API X65 pipeline steel in H_2S containing environment: influence of heat treatment and its subsequent microstructural changes. Journal of Materials Research and Technology, 15, pp. 1-16. DOI: 10.1016/j.jmrt.2021.07.118
[15] Arifin, A., Sahadan, S. N. and Abdullah, S. (2019). Evaluating the contraction value of ferromagnetic material at early fatigue loading stage using magnetic flux leakage signature. IOP Conference Series: Materials Science and Engineering, 606(1). DOI: 10.1088/1757-899X/606/1/012014
[16] Sahadan, S.N., Abdullah, S., Arifin, A. and Singh, S.S.K. (2021). Assessing the magnetic flux leakage contraction parameters for the fatigue life prediction of SAE1045 steel specimens, Structures, 34, pp. 4077-4085. DOI: 10.1016/j.istruc.2021.10.004
[17] Dubov, A.A. and Kolokolnikov, S.M. (2009). Method of Metal Magnetic Memory (MMM) and Inspection Instruments. Ed. ke-2. Germany: International Institute of Welding.
[18] Mohamed, S.A.N., Abdullah, S., Arifin, A., Ariffin, A.K., Padzi, M.M. and Yunoh, M.F.M. (2015). Detection of biaxial fatigue stress concentration zone under magnetic flux leakage signals by using wavelet transform, Proceeding of the 4th International Conference on Frature Fatigue and Wear, 3, pp. 241-246.
[19] Percival, D.B. and Walden, A.T. (2000). Wavelet methods for time series analysis, UK: Cambridge University Press.
[20] Gao, J.H., Wu, R.S. and Wang, B.J. (2001). A new type of analyzing wavelet and its applications for extraction of instantaneous spectrum bandwidth, SEG International Exposition and Annual Meeting, San Antonio, Texas.
[21] Misiti, M., Misiti, Y., Oppenheim, G. and Poggi, J.-M. (2008). Wavelet Toolbox User's Guide, fourth ed., The Math Works Inc, MA.
[22] Purushotham, V., Narayanan, S. and Prasad, S. A. N. (2005). Multi-fault diagnosis of rolling bearing elements using wavelet analysis and hidden Markov model based fault recognition. NDT and E International, 38(8), pp. 654–664. DOI: 10.1016/j.ndteint.2005.04.003
[23] Daubechies, I. (1992). Ten Lectures on Wavelets, Society for Industrial and Applied Mathematics, Philadelphia.
[24] Addison, P.S. (2002). The illustrated wavelet transform handbook, UK: Institute of Physics Publishing.
[25] Venkatachalapathi, N., Basha, S.MD.J., Raju, G.J. and Raghavulu, P. (2018). Characterization of Fatigued Steel States with Metal Magnetic Memory Method, Materials Today: Proceedings 5, pp. 8645-8654.
[26] Kong, Y.S., Abdullah, S., Haris, S.M., Omar, M.Z. and Schramm, D. (2018). Generation of Artificial Road Profile for Automobile Spring Durability Analysis, Jurnal Kejuruteraan, 30(2), pp. 123–128. DOI:10.17576/jkukm-2018-30(2).